Dispersion-free transient-grating frequency-resolved optical gating

Ming Li, John P. Nibarger, Chunlei Guo, and George N. Gibson

We have developed a compact dispersion-free TG (transient-grating) FROG (frequency-resolved optical gating) by utilizing a mask that separates the input beam into three distinct beams focused into fused silica to create the FROG signal. Two of the beams are reflected off the same set of mirrors to ensure identical optical paths, eliminating the difficulty in establishing zero time delay between the beams. In addition, the use of only reflective optics avoids material dispersion in the FROG except for the mixing crystal. This TG FROG is capable of operating with an intensity of 1×10^{11} W/cm^2 and has resolutions less than 0.5 and 1.3 fs for 25- and 10-fs input pulses, respectively. © 1999 Optical Society of America

OCIS codes: 320.0320, 320.7100, 190.1900.

1. Introduction

Frequency-resolved optical gatings (FROG's) have been widely used to characterize short laser pulses to the utmost. Many different FROG devices have been developed by use of various geometries and nonlinear processes, including second-order and third-order wave mixings,[1–4] each with its own advantages and disadvantages. Compared with third-order wave mixing, second-order processes are ambiguous in time and give unintuitive FROG traces. Among third-order configurations, a particularly simple design that is simultaneously phase matched and background free is the transient-grating (TG) FROG.[4,5]

Previous TG FROG designs have two main drawbacks: material dispersion and difficulty in setting the zero time delay between the two fixed pulses. Beam splitters, which are used to create the three separate beams, introduce dispersion,[4] which creates a problem for accurate measurements of pulses with durations below 30 fs. Multiple translation stages have been used to create the zero time delay between the two fixed beams. The accuracy of these stages introduces additional errors into the overall measurement of the pulse. Here we present a novel geometry for the TG FROG that is dispersion free and automatically ensures a zero time delay between two of the beams. Although a similar design was presented in Ref. 6, to our knowledge this is the first time this geometry is used in a FROG design.

The layout of our TG FROG is shown in Fig. 1. A short-pulse laser beam is separated by an input mask (Fig. 2) into three beams, which then travel to a pair of nested retroreflectors. Beams 2 and 3 travel to the inner retroreflectors (M2 and M3) that are positioned on a 0.1-μm/step translation stage (Newport Corp., Irvine, Calif.). The other beam reflects off the outer retroreflectors (M1 and M4). The axes of the two retroreflectors are offset so that both positive and negative time delays are possible. The three beams are then focused by an off-axis 75-mm focal-length parabolic mirror (Janos Corp.) into a piece of 1-mm thick fused silica with a 170-μm-diameter spot size. The output mask shown in Fig. 2 is placed in the image plane of the input mask formed by the parabolic mirror. The FROG signal beam is generated by degenerate four-wave mixing (DFWM) in the fused silica. There are a number of four-wave mixing output beams from our geometric configuration, only one of which is perfectly degenerated and phase matched and is selected with the output mask (Fig. 2). This output beam is then sent to a computer-interfaced spectrometer through a single-mode 7-μm-diameter optical fiber (Ocean Optics, Inc., Dunedin, Fla., Model S2000). There is no dispersive optics prior to the fused silica mixing crystal where the FROG signal is generated. The compact design creates a small overall footprint of only 23 cm × 33 cm.

We verified that the output signal strength is proportional to the cube of the input laser strength.

The authors are with the Department of Physics, University of Connecticut, Storrs, Connecticut 06269. The e-mail address for M. Li is phli@phys.uconn.edu.

Received 25 January 1999; revised manuscript received 9 June 1999.

0003-6935/99/245250-04$15.00/0

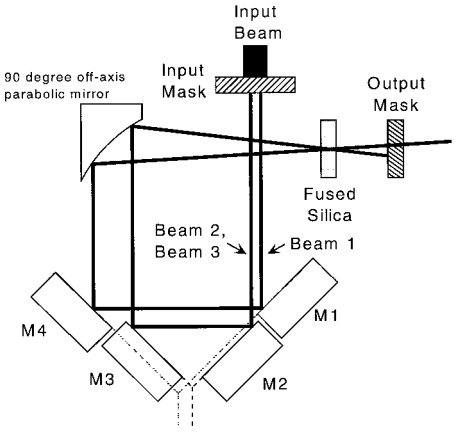

Fig. 1. TG FROG configuration. Beams 2 and 3 are vertically separated. M1 and M4 and M2 and M3 form two pairs of retroreflectors with the inner pair (M2 and M3) on a motorized translation stage.

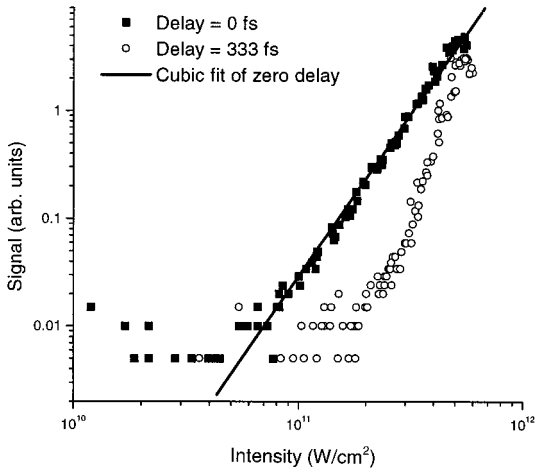

Fig. 3. DFWM FROG signal at zero time delay with a cubic fit. At a time delay of 333 fs, there is no temporal overlap of the fixed and delayed beams. The only signal arises from self-phase modulation of the beam.

Figure 3 shows the cubic dependence when there is zero delay between the fixed and delayed beams. Furthermore, by offsetting the fixed and delayed pulses by 333 fs when there is no overlap in time between them, we measured the onset of self-phase modulation and verified that there is an operational intensity at which the self-phase modulation is negligible. By combining the two curves in Fig. 3, we found that the working intensity is between 0.75 and 3×10^{11} W/cm^2.

The fluctuation of per-pulse energy has a strong effect on the generation of a DFWM signal. Normalization, windowing, and averaging are used to compensate for the fluctuations in laser intensity. A reference diode is set up to monitor the per-pulse laser energy. Its output is integrated by a boxcar (Stanford Research System, Sunnyvale, Calif.) and then sent to a data-acquisition computer for normalization. This process is synchronized with the FROG signal acquisition so that per-pulse normalization is achieved. In the software layer, a window, which consists of a lower bound and an upper bound, is set for the laser reference diode signal. We retained only those pulses that occur in this window. The windowing technique can greatly reduce the effect of fluctuations. Typically, 100 normalized shots are averaged by the program in real time.

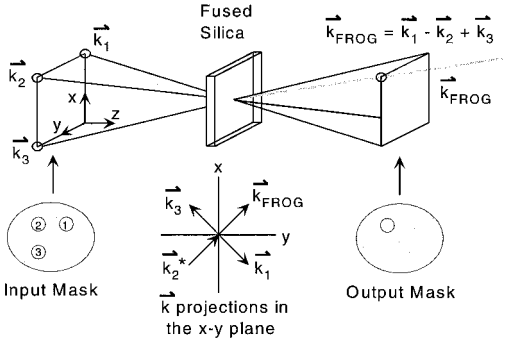

Fig. 2. Input and output mask specifications for DFWM. The $\mathbf{k}_i$ vector corresponds to the ith beam. The input beam is 10 mm × 8 mm and the input mask holes are 1 mm in diameter with a 2-mm center-to-center separation. The output mask hole is 1 mm in diameter and is positioned at the image plane of the input mask.

A TG FROG has the strict requirement of zero time delay between the two fixed beams,[4,5] a condition that is difficult to achieve with a traditional beam splitter design. In our design, the two fixed beams travel the exact same optical path automatically as long as they are aligned parallel to the optical axis of the parabolic mirror, which significantly simplifies the alignment process.

The overall temporal resolution of our FROG is limited by two factors: noncollinearity of the **k** vectors in the DFWM process and discrete motion of the stepper motor. The angle between two **k** vectors is ~1.5°, which gives a blurring term of $t_{blur} = 5.37$ fs for an 800-nm wavelength and a 170-μm spot size. The measured value, $t_{measured}$, and the actual value, t_{actual}, satisfy the following equation:

$$t_{measured} = \sqrt{{t_{actual}}^2 + {t_{blur}}^2}. \quad (1)$$

Based on Eq. (1), we found 2% (0.5 fs) and 13% (1.3 fs) blurring for 25- and 10-fs input pulses, respectively. The stepper motor moves in discrete 0.1-μm steps, yielding a resolution of 0.67 fs, which is negligible.

As shown in Fig. 2, beams 1 and 3 are on a diagonal, whereas beam 2 is off diagonal. The three beams are not all equivalent: off-diagonal beam 2 is unique because its **k** vector is subtracted in the DFWM process, as represented mathematically by the complex conjugate of its electric field. For this reason there are two distinct beam-delaying choices, which in fact lead to two different kinds of FROG trace. The first choice is to keep beams 1 and 3 fixed in time and delay beam 2; the second choice is to group either beam 1 or 3 with beam 2 and delay the

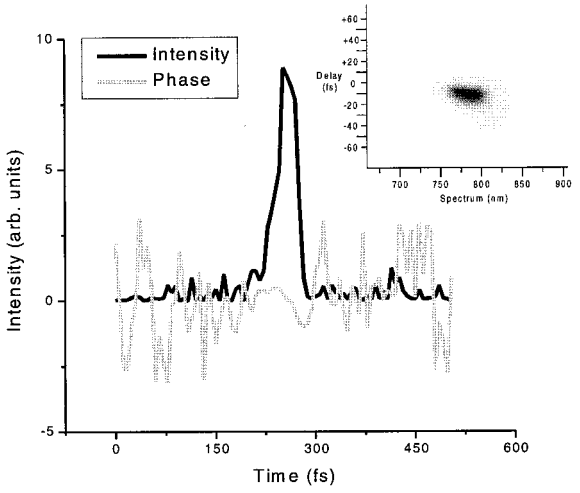

Fig. 4. FROG trace of a near-transform-limited pulse along with its retrieved intensity and phase in the time domain showing a pulse duration of 35 fs.

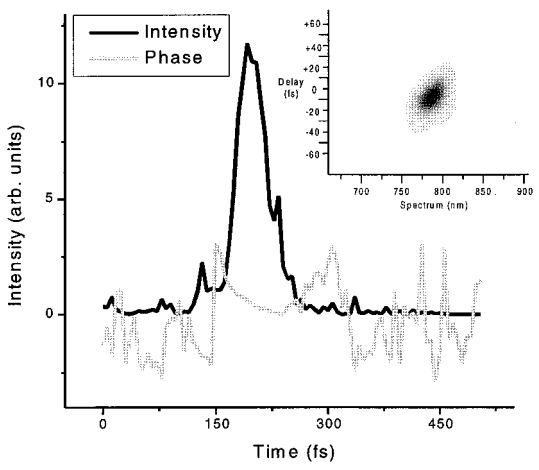

Fig. 5. FROG trace of a linearly chirped pulse along with its retrieved intensity and phase in the time domain showing a pulse duration of 50 fs.

other one. The output FROG traces for these two cases are described by relations (2) and (3), respectively:

$$I_{\text{choice\_1}}(\omega, \tau) \propto \left| \int_{-\infty}^{\infty} E_1(t) E_2^*(t-\tau) E_3(t) \exp(i\omega t) \mathrm{d}t \right|^2, \tag{2}$$

$$I_{\text{choice\_2}}(\omega, \tau) \propto \left| \int_{-\infty}^{\infty} E_1(t-\tau) E_2^*(t) E_3(t) \exp(i\omega t) \mathrm{d}t \right|^2 = \left| \int_{-\infty}^{\infty} E_1(t-\tau) |E_2(t)|^2 \exp(i\omega t) \mathrm{d}t \right|^2, \tag{3}$$

where E_1, E_2, and E_3 are electric fields of beams 1, 2, and 3, respectively, and are of equal magnitude. Relation (3) is a simpler mathematical form than is relation (2), and its retrieval is less complicated. Thus, beam 1, as one of the diagonal beams, was chosen as the delayed beam for our design and, fortunately, can be delayed conveniently.

The laser pulses used for diagnosis were generated by our Ti:sapphire laser system.[7] A FROG trace for 35-fs pulses with zero second-order dispersion is shown in Fig. 4. Figure 5 depicts a trace of linearly chirped pulses. As expected, the trace of unchirped pulses is round and that of chirped pulses is slanted.

To sample the time and frequency domain equally, we had to choose frequency resolution $\mathrm{d}\omega$ and the time-delay step size $\mathrm{d}t$ such that

$$\frac{\mathrm{d}\omega}{\Delta\omega} = \frac{\mathrm{d}t}{\Delta t}, \tag{4}$$

where $\Delta\omega$ and Δt are the bandwidth and pulse duration of the laser. For an $N \times N$ FROG trace, we also have $\mathrm{d}\omega \mathrm{d}t = 1/N$, which gives optimal sampling resolutions:

$$\mathrm{d}\omega = \sqrt{\frac{\Delta\omega}{N\Delta t}}, \qquad \mathrm{d}t = \sqrt{\frac{\Delta t}{N\Delta\omega}}. \tag{5}$$

The FROG traces were retrieved based on the algorithms in Refs. 3 and 8. The retrieved intensity and phase in the time domain are shown in Figs. 4 and 5, respectively. The retrieved pulse durations are ~35 and ~50 fs full width at half-maximum. These results agree with the results obtained from our second-harmonic autocorrelation to within ±10%. One stringent test of our retrieval algorithm was to retrieve two identical pulses with a known time delay because such a retrieval problem is considered to be difficult. Figure 6 shows the FROG trace of two 35-fs pulses separated by 100 fs. The

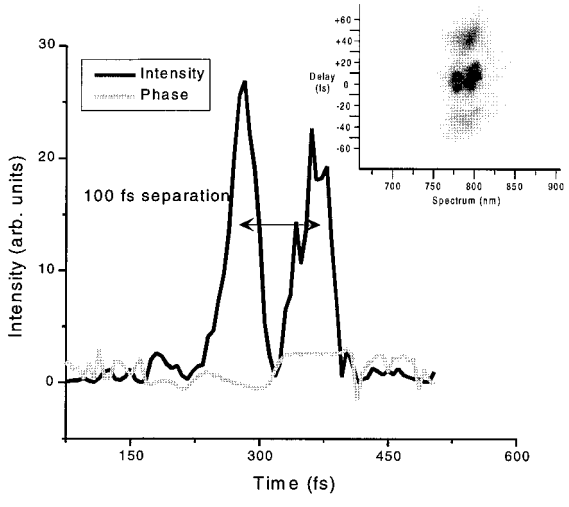

Fig. 6. FROG trace of a pair of near-transform-limited pulses separated by 100 fs along with its retrieved intensity and phase in the time domain.

trace retrieval proves that the time interval between the two retrieved pulses is indeed 100 fs, which demonstrates the robustness of the retrieval algorithm as well as the FROG apparatus in general. This double-pulse technique can also be used to calibrate the system.

With the conventional beam splitter eliminated, the new TG FROG is capable of generating high-resolution FROG traces for ultrashort laser pulses without introducing any dispersion. The unique and compact FROG configuration automatically establishes zero time delay between the fixed beams, simplifying the alignment procedure. The new system requires a slightly higher energy because of the input mask and operates between 0.75 and 3×10^{11} W/cm^2.

The authors acknowledge support from the NSF under grant PHYS 9502935. In addition, G. N. Gibson was also supported through funding as a Cottrell Scholar of the Research Corporation.

References

1. R. Trebino and D. J. Kane, "Using phase retrieval to measure the intensity and phase of ultrashort pulses: frequency-resolved optical gating," J. Opt. Soc. Am. A **10,** 1101–1111 (1993); B. Kohler, V. V. Yakovlev, K. R. Wilson, J. Squier, K. W. DeLong, and R. Trebino, "Phase and intensity characterization of femtosecond pulses from a chirped-pulse amplifier by frequency-resolved optical gating," Opt. Lett. **20,** 483–485 (1995).
2. D. J. Kane and R. Trebino, "Single-shot measurement of the intensity and phase of an arbitrary ultrashort pulse by using frequency-resolved optical gating," Opt. Lett. **18,** 823–825 (1993).
3. K. W. DeLong, R. Trebino, and D. J. Kane, "Comparison of ultrashort-pulse frequency-resolved-optical-gating traces for three common beam geometries," J. Opt. Soc. Am. B **11,** 1595–1608 (1994).
4. J. N. Sweester, D. N. Fittinghoff, and R. Trebino, "Transient-grating frequency-resolved optical gating," Opt. Lett. **22,** 519–521 (1997).
5. H. J. Eichler, P. Gunther, and D. W. Pohl, *Laser-Induced Dynamic Gratings* (Springer-Verlag, Berlin, 1986).
6. M. Versluis, G. Meijer, and D. W. Chandler, "Degenerate four-wave mixing with a tunable excimer laser," Appl. Opt. **33,** 3289–3295 (1994).
7. M. Li and G. N. Gibson, "Flexible aberration-free multipass amplifier and compressor for ultrashort-pulse amplification," J. Opt. Soc. Am. B **15,** 2404–2409 (1998).
8. D. J. Kane and R. Trebino, "Characterization of arbitrary femtosecond pulses using frequency-resolved optical gating," IEEE J. Quantum Electron. **29,** 571–579 (1993); T. Sharp-Clement, A. J. Taylor, and D. J. Kane, "Single-shot measurement of the amplitude and phase of ultrashort laser pulses in the violet," Opt. Lett. **20,** 70–72 (1995).